

The condensation of the corona for the correlation between the hard X-ray photon index Γ and the reflection scaling factor \mathfrak{R} in active galactic nuclei

Erlin Qiao ^{1,2}[★] and B.F. Liu ^{1,2}

¹Key Laboratory of Space Astronomy and Technology, National Astronomical Observatories, Chinese Academy of Sciences, Beijing 100012, China

²School of Astronomy and Space Sciences, University of Chinese Academy of Sciences, 19A Yuquan Road, Beijing 100049, China

Accepted XXX. Received YYY; in original form ZZZ

ABSTRACT

Observationally, it is found that there is a strong correlation between the hard X-ray photon index Γ and the Compton reflection scaling factor \mathfrak{R} in active galactic nuclei. In this paper, we propose that the $\Gamma - \mathfrak{R}$ correlation can be explained within the framework of the condensation of the hot corona onto the cold accretion disc around a supermassive black hole. In the model, it is presumed that, initially, a vertically extended hot gas (corona) is supplied to the central supermassive black hole by capturing the interstellar medium and stellar wind. In this scenario, when the initial mass accretion rate $\dot{M}/\dot{M}_{\text{Edd}} \gtrsim 0.01$, at a critical radius r_d , part of the hot gas begins to condense onto the equatorial disc plane of the black hole, forming an inner cold accretion disc. Then the matter is accreted in the form of the disc-corona structure extending down to the innermost stable circular orbits of the black hole. The size of the inner disc is determined by the initial mass accretion rate. With the increase of the initial mass accretion rate, the size of the inner disc increases, which results in both the increase of the Compton reflection scaling factor \mathfrak{R} and the increase of the hard X-ray photon index Γ . By comparing with a sample of Seyfert galaxies with well-fitted X-ray spectra, it is found that our model can roughly explain the observations. Finally, we discuss the possibility to apply our model to high mass X-ray binaries, which are believed to be fueled by the hot wind from the companion star.

Key words: accretion, accretion discs – black hole physics – galaxies: active

1 INTRODUCTION

The hard X-ray spectra of bright Seyfert galaxies can phenomenologically be described by a power law with a high energy exponential cut off at a few hundred keV, i.e., $F(E) \propto E^{-\Gamma+1} \exp(-E/E_c)$ (with Γ being the hard X-ray photon index, and E_c being the e-folding cut-off energy), plus a reflection component (e.g. [Nandra & Pounds 1994](#)). It is believed that the hard power-law X-ray spectrum is produced by the inverse Compton scattering of the soft photons from a cold accretion disc in an optically thin, hot corona ([Sunyaev & Titarchuk 1980](#)). While the reflection spectrum is generally thought to be produced by the illumination of the cold disc by the hot corona ([White et al. 1988](#); [George & Fabian 1991](#); [Laor 1991](#); [Done et al. 1992](#); [Magdziarz & Zdziarski 1995](#); [Ross & Fabian 2005](#); [Dauser et al. 2010](#); [García et al. 2011, 2013](#)). The relative strength of the reflection component depends on the fraction of the emission of the hot corona intercepted by the cold accretion disc, which is often normalized by a reflection scaling

factor \mathfrak{R} , defined as $\mathfrak{R} = \Omega/2\pi$ (with Ω being the solid angle covered by the accretion disc as seen from the hot corona). Originally, it was found that there is positive correlation between Γ and \mathfrak{R} by analyzing the observational data of *Ginga* for black hole X-ray transient GX 339-4 in the low/hard state ([Ueda et al. 1994](#)), which was confirmed by analyzing the RXTE/PCA data in the low/hard state of GX 339-4 during 1996-1997 ([Revnivtsev et al. 2001](#)). A similar correlation between Γ and \mathfrak{R} was also found in black hole high mass X-ray binary Cyg X-1 ([Gilfanov et al. 1999](#); [Ibragimov et al. 2005](#); [Gilfanov 2010](#), for review). The first report on the correlation between Γ and \mathfrak{R} in active galactic nuclei (AGNs) was by [Magdziarz et al. \(1998\)](#), in the type 1 Seyfert galaxy NGC 5548. Later, this correlation was confirmed by a comprehensive study of a sample, including Seyfert galaxies, radio galaxies and black hole X-ray binaries and weakly magnetized neutron stars ([Zdziarski et al. 1999, 2003](#)). A recent study on a sample of 28 Seyfert galaxies further confirmed this correlation ([Lubiński et al. 2016](#)).

The correlation between Γ and \mathfrak{R} is suggested to be used to explore the geometry of the accretion flow around a supermassive

* E-mail: qiaoe@nao.cas.cn

black hole in AGNs (e.g. [Zdziarski et al. 1999](#)). Generally, it is believed that, for luminous AGNs, mainly including the bright Seyfert galaxies and radio quiet quasars, the accretion mode is a cold accretion disc sandwiched by a hot corona extending down to the innermost stable circular orbits (ISCO) of the central black hole ([Shakura & Sunyaev 1973](#); [Shields 1978](#); [Malkan & Sargent 1982](#); [Elvis et al. 1994](#); [Kishimoto et al. 2005](#); [Shang et al. 2005](#)). In such a disc-corona model, the cold accretion disc mainly contributes to the optical/UV emission, and the hot corona mainly contributes to the X-ray emission. Meanwhile, if the hot corona is assumed to be moving away from or towards the cold accretion disc with a mildly relativistic bulk velocity, the model can well explain the observed correlation between the hard X-ray photon index Γ and the reflection scaling factor \mathfrak{R} ([Beloborodov 1999](#); [Malzac et al. 2001](#)). However, theoretically, in the disc-corona model, the formation of the corona is a big problem. Historically, it was only assumed that a fraction of the matter in the disc is transferred to the coronal region to explain the observed strong X-ray emissions in luminous AGNs (e.g. [Haardt & Maraschi 1991, 1993](#); [Svensson & Zdziarski 1994](#); [Stern et al. 1995](#)). Although some important progresses have been achieved via magnetohydrodynamic (MHD) simulations in the past few decades, it is still in debate currently (e.g. [Miller & Stone 2000](#); [Hirose et al. 2006](#); [Bai & Stone 2013](#); [Fromang et al. 2013](#); [Uzdensky 2013](#); [Takahashi et al. 2016](#)). [Jiang et al. \(2014\)](#) performed a three dimensional radiation MHD simulation, they found that the fraction of the energy dissipated in the corona increases with decreasing the surface density of the accretion disc. However, with a lowest surface density in their simulation, the maximum fraction of the energy dissipated in the corona is only 3.4%, which is inconsistent with the strong X-ray emission often observed in luminous AGNs ([Vasudevan & Fabian 2007, 2009](#)).

As suggested by [Liu et al. \(2015\)](#), the physical properties of the initial gas fuel is important for the X-ray emission for luminous AGNs. In the paper, we interpret the $\Gamma - \mathfrak{R}$ correlation in luminous AGNs within the framework of the condensation of the hot corona onto the cold accretion disc around a supermassive black hole. In this model, it is presumed that, initially, the matter is accreted in the form of vertically extended hot gas (corona) at the region beyond the Bondi radius of the black hole. It is found that, for $M/M_{\text{Edd}} \gtrsim 0.01$ (with $\dot{M}_{\text{Edd}} = 1.39 \times 10^{18} M/M_{\odot} \text{ gs}^{-1}$), when the gas flows towards the central black hole, at a critical radius r_d , a fraction of the hot gas begins to condense onto the equatorial disc plane of the black hole, forming an inner cold accretion disc. Then the gas will be accreted in the form of the disc-corona structure extending down to the ISCO of the black hole. The size of the inner disc is determined by the initial mass accretion rate. With the increase of the initial mass accretion rate, the size of the inner disc increases, which results in both the increase of the Compton reflection scaling factor \mathfrak{R} and the increase of the hard X-ray photon index Γ . By comparing with a sample of Seyfert galaxies with well-fitted X-ray spectra, it is found that our model can roughly explain the observations. Our model is briefly described in Section 2. The numerical results and some comparisons with observations are shown in Section 3. Some discussions are in Section 4, and the conclusions are in Section 5.

2 THE MODEL

Initially, the matter is presumed to be accreted in the form of a vertically extended, optically thin, hot gas (corona) beyond the Bondi radius of the central black hole. One can see the panel a of Fig. 1 for

clarity. We study the interaction between the hot corona and a pre-existing geometrically thin, optically thick, cold accretion disc in the vertical direction. The interaction between the disc and corona leads to either the matter in the accretion disc to be evaporated to the corona or the matter in the corona to be condensed to the disc until a dynamic equilibrium is established between the disc and the corona. We take the vertically stratified method to treat the interaction between the disc and the corona, in which the accretion flow is divided into three parts in the vertical direction, i.e., a hot corona, a thin disc, and a transition layer between them.

2.1 The corona

The corona is treated as a two-temperature hot accretion flow, which is described by the self-similar solution of the advection dominated accretion flow (ADAF) ([Narayan & Yi 1994, 1995](#)). The pressure p , the electron number density n_e , the viscous heating rate q^+ and the isothermal sound speed c_s as functions of black hole mass m , mass accretion rate \dot{m}_c , viscosity parameter α and the magnetic parameter β (defined as $p_m = B^2/8\pi = (1 - \beta)p$, where $p = p_{\text{gas}} + p_m$, with p_{gas} being the gas pressure and p_m being the magnetic pressure) are expressed as ([Narayan & Yi 1995](#)),

$$\begin{aligned} p &= 1.71 \times 10^{16} \alpha^{-1} c_1^{-1} c_3^{1/2} m^{-1} \dot{m}_c r^{-5/2} \text{ g cm}^{-1} \text{ s}^{-2}, \\ n_e &= 2.00 \times 10^{19} \alpha^{-1} c_1^{-1} c_3^{-1/2} m^{-1} \dot{m}_c r^{-3/2} \text{ cm}^{-3}, \\ q^+ &= 1.84 \times 10^{21} \epsilon' c_3^{1/2} m^{-2} \dot{m}_c r^{-4} \text{ ergs cm}^{-3} \text{ s}^{-1}, \\ c_s^2 &= 4.50 \times 10^{20} c_3 r^{-1} \text{ cm}^2 \text{ s}^{-2}, \end{aligned} \quad (1)$$

where m is the black hole mass scaled with the solar mass M_{\odot} , \dot{m}_c is the coronal/ADAF mass accretion rate scaled with the Eddington accretion rate \dot{M}_{Edd} , r is the radius scaled with the Schwarzschild radius R_S (with $R_S = 2.95 \times 10^5 m \text{ cm}$), and

$$\begin{aligned} c_1 &= \frac{(5+2\epsilon')}{3\alpha^2} g(\alpha, \epsilon'), \\ c_3 &= \frac{2\epsilon'(5+2\epsilon')}{9\alpha^2} g(\alpha, \epsilon'), \\ \epsilon' &= \frac{\epsilon}{f} = \frac{1}{f} \left(\frac{5/3-\gamma}{\gamma-1} \right), \\ g(\alpha, \epsilon') &= \left[1 + \frac{18\alpha^2}{(5+2\epsilon')^2} \right]^{1/2} - 1, \\ \gamma &= \frac{32-24\beta-3\beta^2}{24-21\beta}, \end{aligned} \quad (2)$$

with f being the advected fraction of the viscously dissipated energy. The energy balance of the electrons in the corona/ADAF is determined by the following equation,

$$\Delta F_c / H = q_{\text{ie}} - q_{\text{rad}}, \quad (3)$$

where ΔF_c refers to the flux transferred from the upper boundary of the corona/ADAF to the interface of the transition layer. H refers to the height of the corona/ADAF, given by $H = (2.5c_3)^{1/2} r R_S$. q_{ie} refers to the energy transfer rate from ions to electrons ([Stepney 1983](#)), which is re-expressed for a two-temperature hot accretion flow as ([Liu et al. 2002](#)),

$$q_{\text{ie}} = (3.59 \times 10^{-32} \text{ g cm}^5 \text{ s}^{-3} \text{ K}^{-1}) n_e n_i T_i \left(\frac{kT_e}{m_e c^2} \right)^{-3/2}. \quad (4)$$

$q_{\text{rad}}(n_e, T_e) = q_{\text{brem}} + q_{\text{syn}} + q_{\text{cmp}} + q_{\text{excmp}}$ refers to the cooling rate of the electrons in the corona/ADAF, with q_{brem} , q_{syn} and q_{cmp} being the bremsstrahlung cooling rate, synchrotron cooling rate and the

corresponding self-Compton cooling rate respectively. q_{brem} , q_{syn} and q_{cmp} are all the functions of electron number density n_e and electron temperature T_e (Narayan & Yi 1995). q_{excmp} is the Compton cooling rate of the underlying disc photons to the electrons in the corona/ADAF, which is given by

$$q_{\text{excmp}} = \frac{4kT_e}{m_e c^2} n_e \sigma_T c u, \quad (5)$$

with u being the seed photon energy density of the underlying disc. u can be expressed as a function of the distance from the black hole, i.e., $u = \frac{1}{2} a T_{\text{eff}}^4(r) = \frac{1}{2} a \{2.05 T_{\text{eff,max}} (\frac{3}{r})^{3/4} [1 - (\frac{3}{r})^{1/2}]^{1/4}\}^4$ (with a being the radiation constant, $T_{\text{eff,max}}$ being the maximum temperature of the accretion disc). According to the Spitzer's formula for the thermal conduction (Spitzer 1962), i.e., $F_c(z) = k_0 T_e^{5/2} dT_e/dz$, we simply express the conductive flux transferred from the upper boundary of the corona/ADAF to the surface of the transition layer as,

$$\begin{aligned} \Delta F_c &= k_0 T_{\text{em}}^{5/2} (T_{\text{em}} - T_{\text{cpl}}) / H \\ &= k_0 T_{\text{em}}^{7/2} (1 - T_{\text{cpl}}/T_{\text{em}}) / H \\ &\simeq k_0 T_{\text{em}}^{7/2} / H, \end{aligned} \quad (6)$$

where T_{em} refers to the electron temperature at the upper boundary of the corona/ADAF, which is the maximum temperature of the electrons at a fixed radius. T_{cpl} refers to the coupling temperature of the transition layer, which is much less the temperature of the electrons in the corona/ADAF (Meyer et al. 2007; Liu et al. 2007). As demonstrated by Liu et al. (2002), the electron temperature in the main body of corona for a fixed radius is approximately a constant, we simply replace T_{em} by the local temperature T_e .

We solve the equations (1), (3), (4), (5) and (6) for the electron temperature T_e in the corona by specifying m , \dot{m}_c , α , β and the maximum effective temperature of the accretion disc $T_{\text{eff,max}}$. Then we can calculate the flux transferred from the corona/ADAF to the transition layer ΔF_c via equation (6). Meanwhile, if it is presumed that the flux at the upper boundary of the corona/ADAF is approximately zero, the flux arrived at the interface of the transition layer F_c^{ADAF} equals to ΔF_c .

2.2 The transition layer

Following the work of Liu et al. (2007), the energy balance in the transition layer is determined by the incoming energy transferred from the corona/ADAF, the bremsstrahlung radiation, and the enthalpy carried by the mass condensation, which can be expressed as,

$$\frac{d}{dz} \left[\dot{m}_z \frac{\gamma}{\gamma-1} \frac{1}{\beta} \frac{\tilde{\mathfrak{R}} T}{\mu} + F_c \right] = -n_e n_i \Lambda(T), \quad (7)$$

with $\tilde{\mathfrak{R}}$ the gas constant. From equation (7), the condensation/evaporation rate per unit area is given as (Meyer et al. 2007; Liu et al. 2007),

$$\dot{m}_z = \frac{\gamma-1}{\gamma} \beta \frac{-F_c^{\text{ADAF}}}{\tilde{\mathfrak{R}} T_i / \mu_i} (1 - \sqrt{C}), \quad (8)$$

with

$$C \equiv \kappa_0 b \left(\frac{0.25 \beta^2 p_0^2}{k^2} \right) \left(\frac{T_{\text{cpl}}}{F_c^{\text{ADAF}}} \right)^2. \quad (9)$$

From equation (9), setting $C = 1$, a critical radius r_d is determined. From this critical radius inwards, $\dot{m}_z < 0$, indicates that the corona/ADAF matter condenses onto the disc. However, from

this critical radius outwards, $\dot{m}_z > 0$, indicates that the matter evaporates from the disc to the corona/ADAF.

Currently, we don't consider the potential cooling mechanism such as the Compton cooling in the transition layer. Although the Compton cooling in the transition layer should be not very important, as analyzed by Meyer et al. (2007), it will also increase the radiation of the transition layer to some extent. Consequently, the energy transferred from the corona/ADAF to the transition layer will be more easily to be radiated out, an increased amount of the matter will move towards the disc plane, leading to a slight increase of the condensation rate.

2.3 The disc

Combining equations (8) and (9), the integrated condensation rate in units of Eddington rate from R_d to any radius R of the disc inward reads,

$$\dot{m}_{\text{cnd}}(R) = \dot{m}_{\text{disc}}(R) = \int_R^{R_d} \frac{4\pi R}{\dot{M}_{\text{Edd}}} \dot{m}_z dR. \quad (10)$$

According to mass conservation, if the initial mass accretion rate in the corona/ADAF is \dot{m} , the mass accretion rate in the corona is a function of distance,

$$\dot{m}_c(R) = \dot{m} - \dot{m}_{\text{cnd}}(R). \quad (11)$$

The total luminosity of the corona/ADAF is derived by integrating the corona/ADAF region, i.e.,

$$L_{\text{c,t}} = \int_{3R_s}^{R_d} q_{\text{rad}} H 4\pi R dR. \quad (12)$$

2.4 The effect of the irradiation of the disc by the corona

We consider the irradiation of the accretion disc by the corona/ADAF. For simplicity, we assume that the radiation of the corona/ADAF can be regarded as a point source lying above the disc center at a height of H_s . In this case, the reflection scaling factor \mathfrak{R} (equivalent to the covering factor) can be defined as follows,

$$\begin{aligned} \mathfrak{R} &= \frac{\Omega}{2\pi} = \frac{1}{2\pi} \int_{R_{\text{in}}}^{R_d} \frac{H_s}{(R^2 + H_s^2)^{3/2}} 2\pi R dR \\ &= \left[1 + \left(\frac{R_{\text{in}}}{H_s} \right)^2 \right]^{-1/2} - \left[1 + \left(\frac{R_d}{H_s} \right)^2 \right]^{-1/2}, \end{aligned} \quad (13)$$

where R_{in} and R_d are the inner boundary and the outer boundary of the accretion disc respectively. The effective temperature of the accretion disc can be expressed as follows by including both the accretion fed by the condensation and the irradiation of the corona/ADAF,

$$\begin{aligned} T_{\text{eff}}(r) &= 2.05 T'_{\text{eff,max}} \left(\frac{3}{r} \right)^{3/4} \left[1 - \left(\frac{3}{r} \right)^{1/2} \right]^{1/4} \\ &\quad \times \left[\frac{1 + 6L_{\text{c,t}}(1-a)}{\dot{M}_{\text{cnd}} c^2} \frac{H_s}{3R_s} \right]^{1/4} \\ &= 2.05 T_{\text{eff,max}} \left(\frac{3}{r} \right)^{3/4} \left[1 - \left(\frac{3}{r} \right)^{1/2} \right]^{1/4}, \end{aligned} \quad (14)$$

where a is albedo, which is defined as the energy ratio of reflected radiation from the surface of the accretion disc to incident radiation upon it from the corona/ADAF, $T_{\text{eff,max}}$ is expressed as ,

$$T_{\text{eff,max}} = T'_{\text{eff,max}} \left[\frac{1 + 6L_{\text{c,t}}(1-a)}{\dot{M}_{\text{cnd}} c^2} \frac{H_s}{3R_s} \right]^{1/4}. \quad (15)$$

$T'_{\text{eff,max}}$ refers to the maximum effective temperature from disc accretion which is reached at $r_{\text{tmax}} = (49/12)$. The expression of $T'_{\text{eff,max}}$ is given as (Liu et al. 2007),

$$T'_{\text{eff,max}} = 0.2046 \left(\frac{m}{10} \right)^{-1/4} \left[\frac{\dot{m}_{\text{cnd}}(r_{\text{tmax}})}{0.01} \right]^{1/4} \text{ keV}. \quad (16)$$

We calculate the condensation rate of the corona/ADAF from equation (10) and the luminosity of the corona/ADAF from equation (12) by specifying the black hole mass m , the initial mass accretion rate \dot{m} , the viscosity parameter α , magnetic parameter β , the albedo a , the height of the corona/ADAF H_s and a maximum effective temperature of the accretion disc $T_{\text{eff,max}}$. Then a new $T_{\text{eff,max}}$ is derived by combining the equations (10), (12), (15) and (16). We make iterations by changing the value of $T_{\text{eff,max}}$ until a self-consistent solution of the disc and the corona is found, including the size of the inner disc r_d , the condensation rate $\dot{m}_{\text{cnd}}(r)$, the electron temperature of the electrons in the corona/ADAF $T_e(r)$, and the scattering optical depth of the electrons in the corona/ADAF $\tau_{\text{es}}(r)$. With the derived structure of the disc and the corona in radial direction, we calculated the emergent spectrum of the disc-corona system with Monte Carlo simulations, one can refer to Qiao & Liu (2012, 2013) for details.

3 RESULTS

We solve equations (1), (3), (4), (5), (6), (10) (12), (15) and (16) numerically by specifying the black hole mass m , the initial mass accretion rate \dot{m} , the viscosity parameter α , the magnetic parameter β , and the reflection albedo a . In this paper, we set $m = 10^8$. We set $\alpha = 0.3$ as usual (King et al. 2007), and $\beta = 0.95$ as suggested by MHD numerical simulations (Hawley & Krolik 2001). The reflection albedo is relative low, which is suggested to be $a \sim 0.1 - 0.2$ (e.g. Magdziarz & Zdziarski 1995). We fix $a = 0.15$. The height of the corona/ADAF is difficult to determine, as an example, we fix $H_s = 10R_s$.

In the panel a of Fig. 2, we plot the mass accretion rate in the corona and mass accretion rate in the disc as a function of radius from the black hole for different initial mass accretion rates. It is found that the inner disc can be formed when the mass accretion rate $\dot{m} \gtrsim 0.01$. For $\dot{m} = 0.015$, the condensation radius is $r_d = 3.75$. With the increase of the mass accretion rate, the condensation radius increases, i.e., as examples, for $\dot{m} = 0.02, 0.03, 0.05$ and 0.1 the condensations radii are $r_d = 23, 70, 175$ and 444 respectively. One can see the panel b of Fig. 1 for the schematic description for the change of the geometry of the accretion flow with increasing the initial mass accretion rate. Assuming that the black hole is a non-rotating Schwarzschild black hole, so the inner boundary of the accretion disc R_{in} , i.e., the ISCO is $3R_s$. We then calculate the reflection scaling factor \mathfrak{R} with equation (13). The corresponding reflection factors are $\mathfrak{R} = 0.02, 0.56, 0.82, 0.90$, and 0.94 for $\dot{m} = 0.015, 0.02, 0.03, 0.05$ and 0.1 respectively. In the panel b of Fig. 2, we plot the corresponding emergent spectra of the model (not including the reflection spectra). From the bottom up, the mass accretion rates are $\dot{m} = 0.015, 0.02, 0.03, 0.05$ and 0.1 respectively. From the emergent spectra, the hard X-ray photon indices between 2-30 keV are $\Gamma = 1.58, 1.88, 2.01, 2.17$, and 2.29 for $\dot{m} = 0.015, 0.02, 0.03, 0.05$ and 0.1 respectively. It is clear that the hard X-ray photon index Γ increases with increasing \dot{m} , which is consistent with the trend observed in luminous AGNs (e.g. Lu & Yu 1999; Porquet et al. 2004; Wang et al. 2004; Shemmer et al. 2006; Saez et al. 2008; Sobolewska & Papadakis

2009; Cao 2009; Veledina et al. 2011; Liu et al. 2012; Qiao & Liu 2013; Liu et al. 2015).

In our model, in order to simplify the calculation of the irradiation of the accretion disc by the corona/ADAF, we assume that the corona/ADAF is located as a point source above the disc center at a height of H_s . Actually in our model, initially, the matter is accreted in the form with an extended geometry, we should check that the luminosity of the corona/ADAF is indeed compact. In Fig. 3, we plot the ratio between the integrated luminosity of the corona/ADAF from $R_{\text{in}} = 3R_s$ to some radius R and the total luminosity of the corona/ADAF. It can be seen that most of the luminosity of the corona is released in a very narrow region. For example, $R = 10R_s$, $L_c(R/R_s)/L_{c,t} \approx 60\%$, and for $R = 20R_s$, $L_c(R/R_s)/L_{c,t} \approx 80\%$. It is clear that, although the corona/ADAF is geometrically distributed within a wider range in the radial direction, most of the luminosity of the corona/ADAF is still dissipated in a very compact region, which is roughly consistent with our assumption that the corona/ADAF is assumed to be located as a point source above the disc center at the height of $H_s = 10R_s$.

In order to compare with observations for the correlation between Γ and \mathfrak{R} , we search for observational data from literatures. We compiled a sample with 118 Seyfert galaxies by combining two samples from Lubiński et al. (2016) and Zdziarski et al. (2003). In the sample of Lubiński et al. (2016), there are 28 Seyfert galaxies, including 8 type 1, 8 intermediate and 12 type 2 Seyfert galaxies. In the sample of Zdziarski et al. (2003), there are 90 Seyfert galaxies, including 11 radio loud AGNs, and 79 radio quiet AGNs. We fit all the observational data of the 118 sources for the $\Gamma - \mathfrak{R}$ correlation with a second-order polynomial. The best fitting result is expressed as follows,

$$\mathfrak{R} = 3.2 - 5.3\Gamma + 2.1\Gamma^2, \quad (17)$$

one can see the dotted line in the panel a of Fig. 4. We plot our theoretical results for the relation between Γ and \mathfrak{R} as a comparison. One can see the solid red line with five larger red filled circles in the panel a of Fig. 4. The five larger red filled circles from left to right correspond to our theoretical results for $\dot{m} = 0.015, 0.02, 0.03, 0.05$ and 0.1 respectively. It can be seen that our model result can roughly match the case for $\mathfrak{R} \lesssim 1$. We should note that, since we do not consider the effects such as the light bending in the vicinity of the black hole and the relativistic motion of the corona, to the strength of the reflection, the current model intrinsically can only be applied to the case for $\mathfrak{R} \lesssim 1$.

We test the effect of the height of the corona/ADAF H_s to the theoretical relation between Γ and \mathfrak{R} . One can refer to the panel b of Fig. 4. The solid grey line with larger grey circle points refers to the case for $m = 10^8$, $\alpha = 0.3$, $\beta = 0.95$, $a = 0.15$, and $H_s = 3R_s$, and the four points from left to right correspond to $\dot{m} = 0.015, 0.02, 0.05, 0.1$ respectively. The corresponding condensation radii of the four points from left to right are $r_d = 3.7, 6.3, 108, 343$ respectively. The solid black line with larger black circle points refers to the case for $m = 10^8$, $\alpha = 0.3$, $\beta = 0.95$, $a = 0.15$, and $H_s = 20R_s$, and the three points from left to right correspond to $\dot{m} = 0.014, 0.015, 0.02$ respectively. The corresponding condensation radii of the three points from left to right are $r_d = 3.4, 26, 63$ respectively. It is clearly that the assumption for height of the corona/ADAF can affect the relation between Γ and \mathfrak{R} . Theoretically, based on the geometry of the accretion flow in our model, we can more accurately determine the relative location between the disc and corona and then the corresponding strength of the reflection, which is a complicated task to be done in the future, and beyond the current study. On the other hand, observationally, the

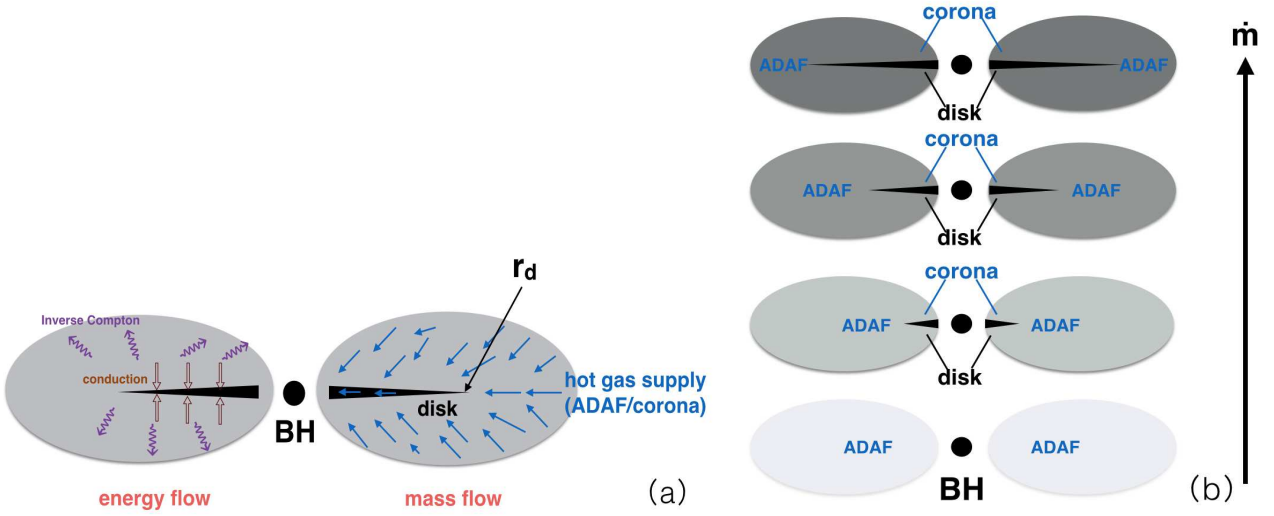


Figure 1.

Panel a: Schematic description of the mass and energy flow in the disc and corona for the initial mass supply with a vertically extended distribution. Panel b: Change of the geometry of the accretion flow with increasing the initial mass accretion rate from the bottom up.

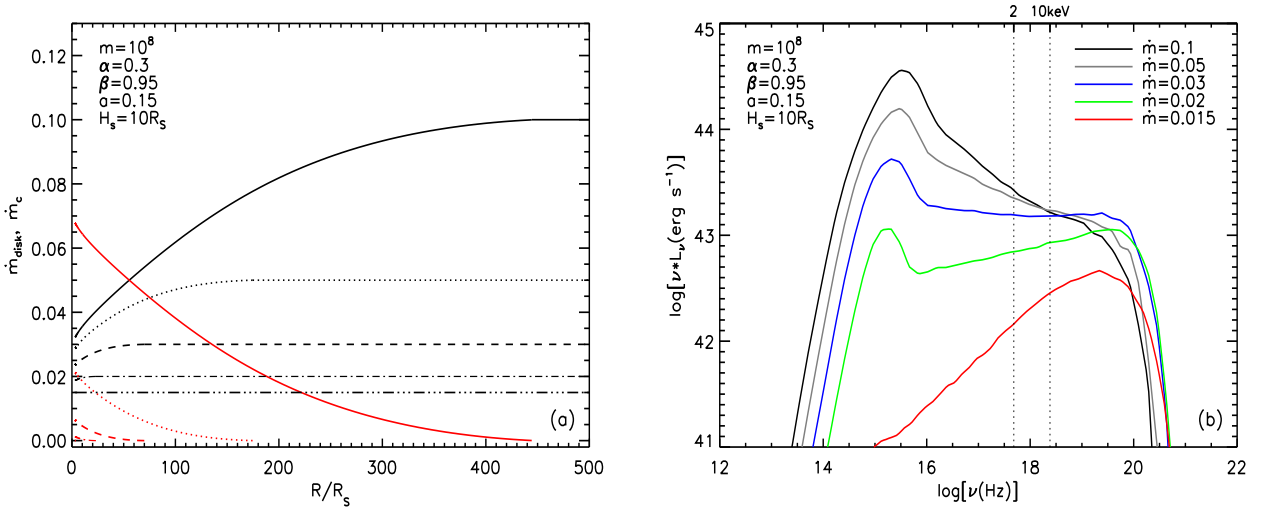


Figure 2.

Panel a: Mass accretion rate in the corona (black line) and mass accretion rate in the accretion disc (red line) as a function of radius. The triple-dotted-dashed line, dotted-dashed line, dashed line, dotted line and the solid line are for $\dot{m} = 0.015, 0.02, 0.03, 0.05$ and 0.1 respectively. In the calculation, we fix $m = 10^8$, $\alpha = 0.3, \beta = 0.95, a = 0.15$ and $H_s = 10R_s$ respectively. Panel b: The corresponding emergent spectra. From the bottom up, the mass accretion rates are $\dot{m} = 0.015, 0.02, 0.03, 0.05$ and 0.1 respectively.

height of the corona can be roughly estimated by some method, like the time lag between the emission in different X-ray bands, which is also roughly consistent with the value we adopted in the calculation (e.g. McHardy et al. 2007; De Marco et al. 2013; Kara et al. 2016).

4 DISCUSSIONS

In the present paper, we proposed a model of the condensation of the corona to explain the observed correlation between the hard X-ray photon index Γ and the reflection scaling factor \mathcal{R} in active galactic nuclei, which is believed to be employed to explore the

geometry of accretion flow around a supermassive black hole. Historically, several models have been proposed to explain such a correlation. Zdziarski et al. (1999) proposed a so-called disc-spheroid model to explain the correlation between Γ and \mathcal{R} . In the disc-spheroid model, an optically thin, hot sphere is surrounded by a flat optically thick accretion disc, which can extend from a truncation radius, $d = 0$ to $d = \infty$, to the black hole. In this model, the seed photons from the cold accretion disc are scattered in the hot sphere, producing the power-law X-ray emission. In turn, a fraction of the power-law X-ray emission from the hot sphere is intercepted by the disc. The intercepted X-ray photons will be partly reflected by the accretion disc, forming the reflection spectrum, and partly be absorbed by the accretion disc, then reprocessed in

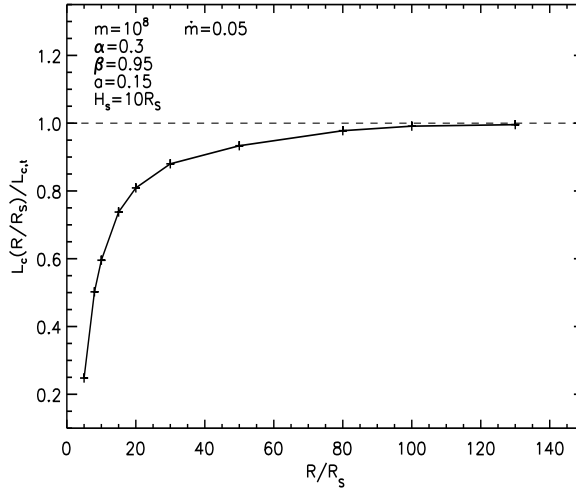


Figure 3.

Ratio between the integrated luminosity of the corona/ADAF from $R_{\text{in}} = 3R_S$ to some radius R , $L_c(R/R_S)$, and the total luminosity of the corona/ADAF $L_{c,t}$ as a function of radius from the black hole.

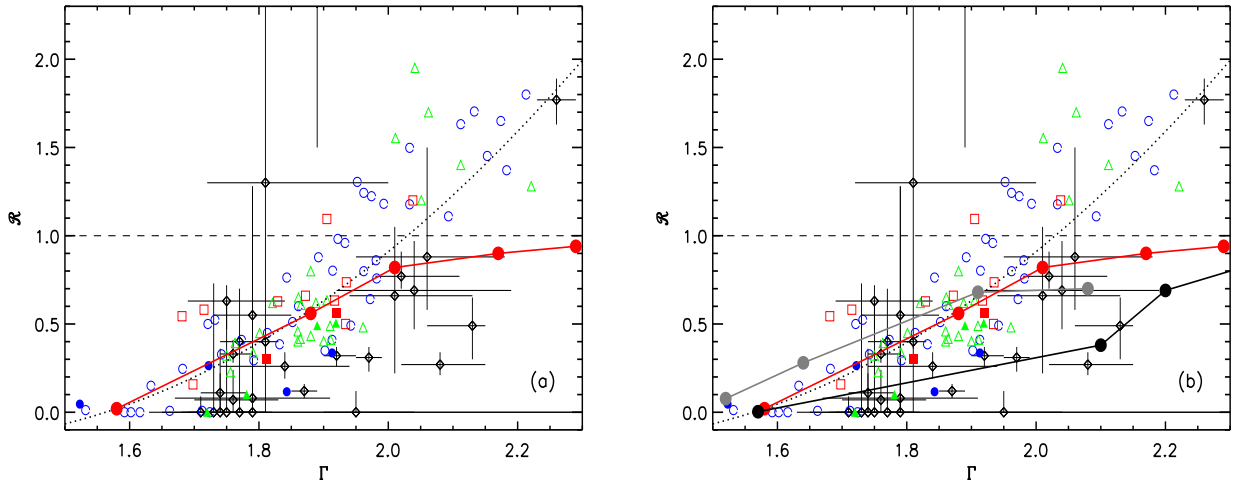


Figure 4.

Panel a: Correlation between the hard X-ray photon index Γ and the reflection scaling factor \mathfrak{R} . The black diamond is a sample composed of 28 Seyfert galaxies, including 8 type 1, 8 intermediate and 12 type 2 Seyfert galaxies, one can refer to [Lubiński et al. \(2016\)](#) for details. The colored small points are from a sample composed of 90 Seyfert galaxies summarized by [Zdziarski et al. \(2003\)](#), including 11 radio loud AGNs (filled symbols), and 79 radio quiet AGNs (Open symbols). The blue circles, green triangles and red squares correspond to the observations by Ginga, RXTE and BeppoSAX respectively. The dotted line refers to the best-fitting result with a second-order polynomial. The red solid line with five larger red filled circles is our theoretical results, and the five larger red filled circles correspond to the model results for $\dot{m} = 0.015, 0.02, 0.03, 0.05$ and 0.1 respectively. In the calculation, we take $m = 10^8$, $\alpha = 0.3$, $\beta = 0.95$, $a = 0.15$ and $H_s = 10R_S$ respectively. Panel b: All the observational data are same with the panel a. We add two sets of theoretical results by assuming different height of the corona. The solid grey line refers to the case for $m = 10^8$, $\alpha = 0.3$, $\beta = 0.95$, $a = 0.15$ and $H_s = 3R_S$. The solid black line refers to the case for $m = 10^8$, $\alpha = 0.3$, $\beta = 0.95$, $a = 0.15$ and $H_s = 20R_S$.

the disc as the seed photons to be scattered in the hot sphere. Finally, a equilibrium feedback between the cold disc and the hot sphere is established. With the decrease of the truncation radius of the accretion disc d , the solid angle covered by the accretion disc as seen from the hot sphere increases, leading to a stronger reflection. Meanwhile, the cooling of the disc to the hot sphere also increases, leading to a softer X-ray spectrum. By changing d arbitrarily from $d = 0$ to $d = \infty$, the model can well reproduce the observed $\Gamma - \mathfrak{R}$ correlation for $\mathfrak{R} \lesssim 1$. We should note that, in [Zdziarski et al.](#)

(1999), the author did not consider the self-Compton scattering of the seed photons (synchrotron radiation and bremsstrahlung) in the hot sphere, which may have obvious effects to the X-ray spectra for the truncation radius of the accretion disc greater than $\sim 30R_S$ ([Poutanen et al. 1997](#); [Esin et al. 1997](#); [Poutanen & Veledina 2014](#), for review).

Theoretically, the physical mechanism of the truncation of the accretion disc has been studied for many years, e.g., the disc evaporation model proposed by [Meyer et al. \(2000a,b\)](#), [Liu et al. \(2002\)](#),

Qiao & Liu (2009, 2010), Qiao et al. (2013), and Taam et al. (2012), or the strong ADAF principle by Narayan & Yi (1995), Abramowicz et al. (1995) and Mahadevan (1997) etc. There are two main findings of the previous studies, (1) the truncation radius of the accretion disc depends on the initial mass accretion rate \dot{m} , i.e., the truncation radius decreases with increasing \dot{m} ; (2) there exists a critical mass accretion rate $\dot{m}_{\text{crit}} \sim \alpha^2$. When $\dot{m} \gtrsim \dot{m}_{\text{crit}}$, the accretion disc does not truncate, and extends down to the ISCO of the black hole. In this case, due to the strong Compton cooling of the seed photons from the accretion disc to the corona, the viscous heating of the corona itself can not sustain the existence of the corona. The corona collapses very quickly, and the accretion will be dominated by the cold accretion disc. Consequently the corona above the disc is too weak to explain the observed power-law hard X-ray emission, not to mention the reflection, unless another heating mechanism (probably the magnetic reconnection heating) for the corona is considered, which is still not very clear (e.g. Meyer-Hofmeister et al. 2012). With these two restrictions, it is unclear whether the correlation between Γ and \mathfrak{R} can still be reproduced well.

Based on the disc evaporation model, Taam et al. (2012) investigated the truncation radius of the accretion disc as functions of α , β and \dot{m} . The author formulized the expression of the truncation radius as,

$$r_{\text{tr}} \approx 17.3\dot{m}^{-0.886}\alpha^{0.07}\beta^{4.61}. \quad (18)$$

It is clear that the strength of the magnetic field, i.e., β , is important to the truncation radius of the accretion disc. Meanwhile, the critical mass accretion rate and the corresponding truncation radius can be expressed as,

$$\dot{m}_{\text{crit}} \approx 0.38\alpha^{2.34}\beta^{-0.41} \quad (19)$$

$$r_{\text{min}} \approx 18.80\alpha^{-2.00}\beta^{4.97}. \quad (20)$$

By changing α , β and \dot{m} , especially β , the model can fit the truncation of the accretion disc for most of low-luminosity AGNs and the black hole X-ray binaries in there low/hard spectral state very well (Gilfanov et al. 2000; Taam et al. 2012; Plant et al. 2015; De Marco et al. 2015; Basak & Zdziarski 2016). However, we notice that, for example, taking $\alpha = 0.3$ and $\beta = 0.95$, the predicted minimum truncation radius is $r_{\text{min}} = 162$; taking $\alpha = 0.3$ and $\beta = 0.8$, the predicted minimum truncation radius is $r_{\text{min}} = 69$. The maximum reflection scaling factors predicted by the above two sets of parameters are $\mathfrak{R}_{\text{max}} = 0.05$ and $\mathfrak{R}_{\text{max}} = 0.13$ respectively, which are too weak to explain the strength of the reflection in a wider range of $\mathfrak{R} \gtrsim \mathfrak{R}_{\text{max}}$. If an extreme value of $\beta = 0.5$ is adopted, the predicted minimum truncation radius $r_{\text{min}} = 6.7$, then $\mathfrak{R}_{\text{max}} = 0.8$, which indeed can extend the reflection in a wider range. However, as the author stressed, the effect of such a strong magnetic field to the structure of the corona is still unclear, which probably makes some assumptions in the model not work. For example, in the model Spitzer's formula is used for the description of the electron thermal conduction in the corona. If a strong magnetic field is considered, Spitzer's formula may not work, which makes the results predicted by the model very uncertain (Meyer & Meyer-Hofmeister 2002). More studies by considering the detailed morphology of the magnetic field or other unknown physical mechanism are still needed to reproduce smaller truncation radii in the future to extend the strength of the reflection in a wider range.

In this work, throughout the calculation, we assume the central black hole as a non-rotating Schwarzschild black hole with the

ISCO being $3R_S$, and we don't consider the effect of the spin of the central black hole to our results. For an extremely rotating Kerr black hole, the accretion disc can extend down to the ISCO being $1/2R_S$, which theoretically can increase the strength of the reflection. Meanwhile, in the vicinity of the black hole, the effect of light bending can also increase the strength of the reflection, which probably can help to explain the case for $\mathfrak{R} \gtrsim 1$ (e.g. Fabian & Vaughan 2003; Reynolds & Nowak 2003; Dauser et al. 2014; Garca et al. 2013). In this work, as the first step, we simply suggested that the condensation of the corona can increase the strength of the reflection, then can explain the observed Γ - \mathfrak{R} correlation for $\mathfrak{R} \lesssim 1$. The study of the effects such as the spin of the black hole, the light bending to the reflection is very complicated, which is beyond the scope of the current work.

We should notice that, in the AGNs case, the scattering of the X-ray emission by the outer torus can also contribute to the reflection. Currently, it is difficult to distinguish the contribution of the disc and torus to the reflection except for some X-ray very bright sources, such as NGC 4151 (Lubiński et al. 2010). Meanwhile, since most of the sources in our sample are type 1 Seyfert galaxies, due to the relative smaller viewing angle, the contribution of the torus to the reflection should be not very important.

We suggest that our model can also be applied to the high mass X-ray binaries (HMXBs). In HMXBs, the companion star is a massive, bright O or B star. A fraction of the matter from the companion star is captured by the compact object via the stellar wind rather than the Roche lobe overflow (RLO) as in the low mass X-ray binaries (LMXBs) (also called X-ray transients). So it is reasonable that, initially, the accreted matter should be in the form of a vertically, extended hot gas in HMXBs rather than be constrained in a very narrow equatorial plane in LMXBs. Since the hot gas is fully ionized, it can not trigger the ionization instability (viscous instability) often observed in LMXBs, which can help us to understand why HMXBs are often relatively stable and the LMXBs are often unstable (e.g. Lasota 2001; Shakura et al. 2015).

5 CONCLUSIONS

In the work, we proposed a model within the framework of the condensation of the corona/ADAF to interpret the observed correlation between the hard X-ray photon index Γ and the reflection scaling factor \mathfrak{R} in AGNs. In the model, beyond the Bondi radius the matter is assumed to be accreted in the form of a vertically extended, hot gas by capturing the interstellar medium and stellar wind. Within this framework, when $\dot{M}/\dot{M}_{\text{Edd}} \gtrsim 0.01$, at a critical radius r_d , a fraction of the accreted hot gas can condense onto the equatorial disc plane, forming an inner disk. Then the accretion will occur in the form a disk-corona system flowing towards the black hole. We found that the size of the inner disk increases with increasing the initial mass accretion rate. With the geometry of the accretion flow, we calculate the reflection scaling factor \mathfrak{R} . Meanwhile, we calculate the emergent spectrum with the structure of the disc and the corona for the hard X-ray photon index Γ . By comparing with the observations of a sample with 118 Seyfert galaxies, it is found that our theoretical relation between Γ and \mathfrak{R} can roughly match the observations for $\mathfrak{R} \lesssim 1$. Finally, we suggested that the current model can be applied to HMXBs, which are believed to be fueled by the hot wind from the bright O or B companion star.

ACKNOWLEDGMENTS

We thank professor W.M. Yuan from NAOC and Professor R.E. Taam from ASIAA for very useful discussions and suggestions. E.L.Qiao thanks the very useful discussions with Dr. M. Gilfanov when visiting Max-Planck Institute for Astrophysics. This work is supported by the National Natural Science Foundation of China (Grants 11303046 and 11673026), the gravitational wave pilot B (Grants No. XDB23040100), and the National Program on Key Research and Development Project (Grant No. 2016YFA0400804).

REFERENCES

- Abramowicz M. A., Chen X., Kato S., Lasota J.-P., Regev O., 1995, *ApJ*, **438**, L37
- Bai X.-N., Stone J. M., 2013, *ApJ*, **767**, 30
- Basak R., Zdziarski A. A., 2016, *MNRAS*, **458**, 2199
- Beloborodov A. M., 1999, *ApJ*, **510**, L123
- Cao X., 2009, *MNRAS*, **394**, 207
- Dauser T., Wilms J., Reynolds C. S., Brenneman L. W., 2010, *MNRAS*, **409**, 1534
- Dauser T., García J., Parker M. L., Fabian A. C., Wilms J., 2014, *MNRAS*, **444**, L100
- De Marco B., Ponti G., Miniutti G., Belloni T., Cappi M., Dadina M., Muñoz-Darias T., 2013, *MNRAS*, **436**, 3782
- De Marco B., Ponti G., Muñoz-Darias T., Nandra K., 2015, *ApJ*, **814**, 50
- Done C., Mulchaey J. S., Mushotzky R. F., Arnaud K. A., 1992, *ApJ*, **395**, 275
- Elvis M., et al., 1994, *ApJS*, **95**, 1
- Esin A. A., McClintock J. E., Narayan R., 1997, *ApJ*, **489**, 865
- Fabian A. C., Vaughan S., 2003, *MNRAS*, **340**, L28
- Fromang S., Latter H., Lesur G., Ogilvie G. I., 2013, *A&A*, **552**, A71
- García J., Kallman T. R., Mushotzky R. F., 2011, *ApJ*, **731**, 131
- García J., Dauser T., Reynolds C. S., Kallman T. R., McClintock J. E., Wilms J., Eikmann W., 2013, *ApJ*, **768**, 146
- George I. M., Fabian A. C., 1991, *MNRAS*, **249**, 352
- Gilfanov M., 2010, in Belloni T., ed., *Lecture Notes in Physics*, Berlin Springer Verlag Vol. 794, *Lecture Notes in Physics*, Berlin Springer Verlag, p. 17 ([arXiv:0909.2567](https://arxiv.org/abs/0909.2567)), doi:10.1007/978-3-540-76937-8_2
- Gilfanov M., Churazov E., Revnivtsev M., 1999, *A&A*, **352**, 182
- Gilfanov M., Churazov E., Revnivtsev M., 2000, *MNRAS*, **316**, 923
- Haardt F., Maraschi L., 1991, *ApJ*, **380**, L51
- Haardt F., Maraschi L., 1993, *ApJ*, **413**, 507
- Hawley J. F., Krolik J. H., 2001, *ApJ*, **548**, 348
- Hirose S., Krolik J. H., Stone J. M., 2006, *ApJ*, **640**, 901
- Ibragimov A., Poutanen J., Gilfanov M., Zdziarski A. A., Shrader C. R., 2005, *MNRAS*, **362**, 1435
- Jiang Y.-F., Stone J. M., Davis S. W., 2014, *ApJ*, **784**, 169
- Kara E., Alston W. N., Fabian A. C., Cackett E. M., Uttley P., Reynolds C. S., Zoghbi A., 2016, *MNRAS*, **462**, 511
- King A. R., Pringle J. E., Livio M., 2007, *MNRAS*, **376**, 1740
- Kishimoto M., Antonucci R., Blaes O., 2005, *MNRAS*, **364**, 640
- Laor A., 1991, *ApJ*, **376**, 90
- Lasota J.-P., 2001, *New Astron. Rev.*, **45**, 449
- Liu B. F., Mineshige S., Meyer F., Meyer-Hofmeister E., Kawaguchi T., 2002, *ApJ*, **575**, 117
- Liu B. F., Taam R. E., Meyer-Hofmeister E., Meyer F., 2007, *ApJ*, **671**, 695
- Liu J. Y., Liu B. F., Qiao E. L., Mineshige S., 2012, *ApJ*, **754**, 81
- Liu B. F., Taam R. E., Qiao E., Yuan W., 2015, *ApJ*, **806**, 223
- Lu Y., Yu Q., 1999, *ApJ*, **526**, L5
- Lubiński P., Zdziarski A. A., Walter R., Paltani S., Beckmann V., Soldi S., Ferrigno C., Courvoisier T. J.-L., 2010, *MNRAS*, **408**, 1851
- Lubiński P., et al., 2016, *MNRAS*, **458**, 2454
- Magdziarz P., Zdziarski A. A., 1995, *MNRAS*, **273**, 837
- Magdziarz P., Blaes O. M., Zdziarski A. A., Johnson W. N., Smith D. A., 1998, *MNRAS*, **301**, 179
- Mahadevan R., 1997, *ApJ*, **477**, 585
- Malkan M. A., Sargent W. L. W., 1982, *ApJ*, **254**, 22
- Malzac J., Beloborodov A. M., Poutanen J., 2001, *MNRAS*, **326**, 417
- McHardy I. M., Arévalo P., Uttley P., Papadakis I. E., Summons D. P., Brinkmann W., Page M. J., 2007, *MNRAS*, **382**, 985
- Meyer F., Meyer-Hofmeister E., 2002, *A&A*, **392**, L5
- Meyer-Hofmeister E., Liu B. F., Meyer F., 2012, *A&A*, **544**, A87
- Meyer F., Liu B. F., Meyer-Hofmeister E., 2000a, *A&A*, **354**, L67
- Meyer F., Liu B. F., Meyer-Hofmeister E., 2000b, *A&A*, **361**, 175
- Meyer F., Liu B. F., Meyer-Hofmeister E., 2007, *A&A*, **463**, 1
- Miller K. A., Stone J. M., 2000, *ApJ*, **534**, 398
- Nandra K., Pounds K. A., 1994, *MNRAS*, **268**, 405
- Narayan R., Yi I., 1994, *ApJ*, **428**, L13
- Narayan R., Yi I., 1995, *ApJ*, **452**, 710
- Plant D. S., Fender R. P., Ponti G., Muñoz-Darias T., Coriat M., 2015, *A&A*, **573**, A120
- Porquet D., Reeves J. N., O'Brien P., Brinkmann W., 2004, *A&A*, **422**, 85
- Poutanen J., Veledina A., 2014, *Space Sci. Rev.*, **183**, 61
- Poutanen J., Krolik J. H., Ryde F., 1997, *MNRAS*, **292**, L21
- Qiao E., Liu B. F., 2009, *PASJ*, **61**, 403
- Qiao E., Liu B. F., 2010, *PASJ*, **62**, 661
- Qiao E., Liu B. F., 2012, *ApJ*, **744**, 145
- Qiao E., Liu B. F., 2013, *ApJ*, **764**, 2
- Qiao E., Liu B. F., Panessa F., Liu J. Y., 2013, *ApJ*, **777**, 102
- Revnivtsev M., Gilfanov M., Churazov E., 2001, *A&A*, **380**, 520
- Reynolds C. S., Nowak M. A., 2003, *Phys. Rep.*, **377**, 389
- Ross R. R., Fabian A. C., 2005, *MNRAS*, **358**, 211
- Saez C., Chartas G., Brandt W. N., Lehmer B. D., Bauer F. E., Dai X., Garmire G. P., 2008, *AJ*, **135**, 1505
- Shakura N. I., Sunyaev R. A., 1973, *A&A*, **24**, 337
- Shakura N. I., Postnov K. A., Kochetkova A. Y., Hjalmarsdotter L., Sidoli L., Paizis A., 2015, *Astronomy Reports*, **59**, 645
- Shang Z., et al., 2005, *ApJ*, **619**, 41
- Shemmer O., Brandt W. N., Netzer H., Maiolino R., Kaspi S., 2006, *ApJ*, **646**, L29
- Shields G. A., 1978, *Nature*, **272**, 706
- Sobolewska M. A., Papadakis I. E., 2009, *MNRAS*, **399**, 1597
- Spitzer L., 1962, *Physics of Fully Ionized Gases*
- Stepney S., 1983, *MNRAS*, **202**, 467
- Stern B. E., Poutanen J., Svensson R., Sikora M., Begelman M. C., 1995, *ApJ*, **449**, L13
- Svensson R., Zdziarski A. A., 1994, *ApJ*, **436**, 599
- Taam R. E., Liu B. F., Yuan W., Qiao E., 2012, *ApJ*, **759**, 65
- Takahashi H. R., Ohsuga K., Kawashima T., Sekiguchi Y., 2016, *ApJ*, **826**, 23
- Ueda Y., Ebisawa K., Done C., 1994, *PASJ*, **46**, 107
- Uzdensky D. A., 2013, *ApJ*, **775**, 103
- Vasudevan R. V., Fabian A. C., 2007, *MNRAS*, **381**, 1235
- Vasudevan R. V., Fabian A. C., 2009, *MNRAS*, **392**, 1124
- Veledina A., Vurm I., Poutanen J., 2011, *MNRAS*, **414**, 3330
- Wang J.-M., Watarai K.-Y., Mineshige S., 2004, *ApJ*, **607**, L107
- White T. R., Lightman A. P., Zdziarski A. A., 1988, *ApJ*, **331**, 939
- Zdziarski A. A., Lubiński P., Smith D. A., 1999, *MNRAS*, **303**, L11
- Zdziarski A. A., Lubiński P., Gilfanov M., Revnivtsev M., 2003, *MNRAS*, **342**, 355

This paper has been typeset from a \LaTeX file prepared by the author.